




Evaluation of the Relationship Between Coral Damage and Tsunami Dynamics; Case Study: 2009 Samoa Tsunami

DERYA I. DILMEN,^{1,2}  VASILY V. TITOV,^{1,2} and GERARD H. ROE²

Abstract—On September 29, 2009, an $M_w = 8.1$ earthquake at 17:48 UTC in Tonga Trench generated a tsunami that caused heavy damage across Samoa, American Samoa, and Tonga islands. Tutuila island, which is located 250 km from the earthquake epicenter, experienced tsunami flooding and strong currents on the north and east coasts, causing 34 fatalities (out of 192 total deaths from this tsunami) and widespread structural and ecological damage. The surrounding coral reefs also suffered heavy damage. The damage was formally evaluated based on detailed surveys before and immediately after the tsunami. This setting thus provides a unique opportunity to evaluate the relationship between tsunami dynamics and coral damage. In this study, estimates of the maximum wave amplitudes and coastal inundation of the tsunami are obtained with the MOST model (TITOV and SYNOLAKIS, J. Waterway Port Coast Ocean Eng: pp 171, 1998; TITOV and GONZALEZ, NOAA Tech. Memo. ERL PMEL 112:11, 1997), which is now the operational tsunami forecast tool used by the National Oceanic and Atmospheric Administration (NOAA). The earthquake source function was constrained using the real-time deep-ocean tsunami data from three DART[®] (Deep-ocean Assessment and Reporting for Tsunamis) systems in the far field, and by tide-gauge observations in the near field. We compare the simulated run-up with observations to evaluate the simulation performance. We present an overall synthesis of the tide-gauge data, survey results of the run-up, inundation measurements, and the datasets of coral damage around the island. These data are used to assess the overall accuracy of the model run-up prediction for Tutuila, and to evaluate the model accuracy over the coral reef environment during the tsunami event. Our primary findings are that: (1) MOST-simulated run-up correlates well with observed run-up for this event ($r = 0.8$), it tends to underestimate amplitudes over coral reef environment around Tutuila (for 15 of 31 villages, run-up is underestimated by more than 10 %; in only 5 was run-up overestimated by more than 10 %), and (2) the locations where the model underestimates run-up also tend to have experienced heavy or very heavy coral damage (8 of the 15 villages), whereas well-estimated run-up locations characteristically experience low or very low damage (7 of 11 villages). These findings imply that a numerical model may overestimate the energy loss of the tsunami waves during their

interaction with the coral reef. We plan future studies to quantify this energy loss and to explore what improvements can be made in simulations of tsunami run-up when simulating coastal environments with fringing coral reefs.

Key words: Tsunami, Samoa, Tutuila, MOST, coral, reef, 2009, Tonga.

1. Introduction

Large tsunamis can wreak devastation upon the near-shore environment. There is abundant documentation of the impacts on the subaerial portion of that environment, but much less on the impacts on the submarine portion. In many tropical settings, coral reefs form an important component of the submarine environment, being the cornerstone of the local ecosystems, as well as shaping the near-shore bathymetry. There is thus the potential for two-way interactions between reefs and tsunamis. The reef bathymetry influences the tsunami dynamics; and tsunami events may cause significant damage to fragile coral structures. In this study, we report on a unique opportunity to document tsunami-related damage, and to evaluate whether the damage can be straightforwardly related to particular aspects of the tsunami dynamics.

On 29 September 2009 at 17:48 UTC, an $M_w 8.1$ earthquake occurred along Tonga-Kermadec Trench. A complicated fault rupture produced bottom deformations and resulted in tsunami waves that generated localized run-ups exceeding 17 m on the island of Tutuila. These waves claimed 34 lives (out of total 192 deaths for the event) and caused extensive damage around the island. The tsunami was detected by coastal tide gauges and offshore sea-level sensors

¹ Pacific Marine Environmental Laboratory, NOAA Center for Tsunami Research, Seattle, USA. E-mail: dilmen@uw.edu; vasily.titov@noaa.gov

² Department of Earth and Space Sciences, University of Washington, Seattle, USA. E-mail: groe@uw.edu

located in Pacific Ocean. The tectonic setting of the Tonga Trench has produced several tsunamis during past hundred years (OKAL *et al.* 2011).

Following the September 29, 2009 tsunami, field surveys were conducted (FRITZ *et al.* 2011) to document the relationship between the physical near-shore environment and the tsunami impact. According to survey results, the tsunami produced a maximum run-up of 17 m at Poloa on the western coast of Tutuila, 12 m at Fagasa on the northern coast, and 10 m at Tula on the eastern coast. The survey team recorded large variations in the impacts of the tsunami along the coastal bays: a wide range of tsunami run-ups, wave directions and inundation. The high degree of spatial variability in these various tsunami fields was somewhat of a surprise to scientists studying the event (FRITZ *et al.* 2011; OKAL *et al.* 2010; BEAVAN *et al.* 2010; ROEBER *et al.* 2010), but was clearly established in the field surveys and confirmed by residents.

The impact of this tsunami on Tutuila has proven unusually hard to simulate in numerical models (BEAVAN *et al.* 2010; OKAL *et al.* 2010; ROEBER *et al.* 2010; FRITZ *et al.* 2011; ZHOU *et al.* 2012). The discrepancies between observations and models have been variously attributed to many factors, including the low-resolution bathymetry and topography, wave dispersion effects, the possibility of resonance over the coral reefs, but most importantly, the unusual complexity of the tsunami source mechanism that may have included multiple ruptures of several fault systems at the same time (BEAVAN *et al.* 2010). We also perform a simulation of this event, and aim to build upon the experience of these earlier studies: we try to eliminate any bathymetric and topographic discrepancies by using a very high-resolution (10 m) dataset (LIM *et al.* 2009); further, we optimize the tsunami source function by calibrating it with direct tsunami observations. Both far-field pressure sensors (DARTs) and near-field coastal sea-level stations (tide gauges) were used to calibrate the tsunami source for this event. We establish good agreement with the near-field tide gauges (Sect. 3), which means it is unlikely that additional details in the source function would impact the simulation.

One challenge of modeling tsunamis in tropical settings such as this are the pervasive barrier and fringing coral reefs, which create tremendous

complexity in bathymetry and topography (Fig. 1). The impact of reefs in tsunami dynamics has been a topic of discussion in the literature. Such analyses point to a complex picture, and conclusions can occasionally appear contradictory. BABA *et al.* (2008) performed numerical simulations of the 2007 Solomon islands Tsunami to explore the effect of Great Barrier Reef (GBR) on tsunami wave height, using the low-resolution bathymetry and ignoring sea-bottom friction and wave dispersion. The results indicate reefs decrease the tsunami wave height due to the refraction and reflection. KUNKEL *et al.* (2006) performs 1D and 2D numerical modeling of tsunami run-up for an idealized island with barrier reefs around the island, and shows that coral reefs reduce tsunami run-up by order of 50 %. However the KUNKEL *et al.* (2006) simulations also suggest the possibility that gaps between adjacent reefs can result in flow amplification and actually increase local wave heights. FERNANDO *et al.* (2005, 2008) lend support to these numerical results: coral reefs protect coastline behind them but local absences of reefs cause local flow amplification due to gaps. Their results are based on field observations, laboratory measurements (FERNANDO *et al.* 2008), and interviews done by local people in Sri Lanka after the 2004 Indian Ocean tsunami. However their laboratory simulations treated corals as a submerged porous barrier made of a uniform array of rods, which likely oversimplifies the complex structural distribution of coral reefs.

Other studies find no effect, or even suggest the opposite conclusions (KUNKEL *et al.* 2006). Based on quantitative field observations of coral assemblages at less than 2 m depth in Aceh after the 2004 Sumatra–Andaman tsunami, BAIRD *et al.* (2005) conclude that the limit of inundation at any particular location is determined by a combination of wave height and coastal topography, and is independent of the reef quality or development prior to the tsunami. Further, CHATENOUX and PEDUZZI (2007) perform statistical and observational analysis of 56 sites located in Indonesia, Thailand, India, Sri Lanka and Maldives with a coarse resolution bathymetry and qualitative coral damage data. They find that the higher the percentage of the corals, the larger the inundation distances behind coral reef on the coast. Lastly, ROEBER *et al.* (2010) identify strong correlations

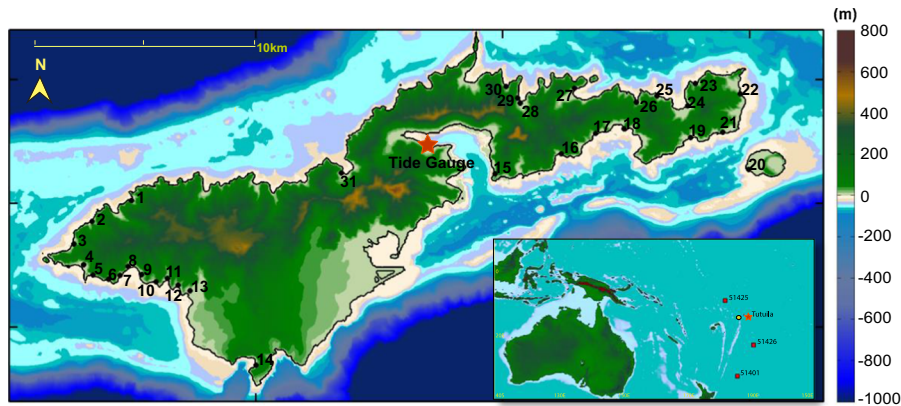


Figure 1

Tutuila island. The beige and light purple colors show the location of the fringing and barrier reefs. The location of Tutuila island is given as red star on the lower right map. The yellow dot on the same map shows the epicenter of the 2009 Samoa earthquake. In the inset panel the location of the DART buoys used in optimizing the earthquake fault source used in the MOST simulations are shown. In the main panel, the location of the PagoPago Tide gauge in Tutuila is shown as red star

between the high variability of run-up and inundation along bays at Tutuila during the 2009 Samoa tsunami with the geomorphology of the island, and suggest a role for high concentrations of resonance energy within particular bays. All of these locations of high-energy concentration have fringing reefs extending 100–200 m from the shores. Based on their tsunami simulations, they hypothesize that fringing reefs might amplify near-shore tsunami energy and worsen the impact of short-period dispersive waves.

In this paper, wave heights, inundation at the coast, and tsunami wave dynamics are simulated for the island of Tutuila for the 2009 tsunami. The simulations are compared with field observations at the coast and wave pressure gauges (DARTs) located around Tutuila to find a relationship between coral damage and coastal metrics of tsunami dynamics. The results contribute to an ongoing discussion about how tsunami dynamics impact corals and how, in turn, that damage might potentially be used to constrain tsunami simulations.

The remainder of the paper is organized as follows: Section 2 describes the study area, the earthquake and tsunami event, and the observational datasets. Section 3 describes the numerical modeling of the earthquake source and the subsequent tsunami. Section 4 presents an analysis of the relationships among the observations, datasets and simulated

tsunami fields. We conclude with a summary and discussion that suggests an outline for future research directions.

2. Study Area and Observations

2.1. Tutuila Island

The study area for this research is Tutuila Island, in American Samoa, the United States' southernmost territory. The Samoa island chain in the central South Pacific Ocean includes five islands, of which Tutuila is the largest and also its center of the government. It is located at roughly 14° south of the equator between longitudes 169° and 173° west (see Fig. 1). The following will summarize some aspects of the geometry of Tutuila island that created unique challenges in modeling of the tsunami.

The island formed in the late Quaternary period, from oceanic crust as the Pacific tectonic plate moved over a hotspot (TERRY *et al.* 2005). Due to its volcanic formation, it has rocky, steep topography and bathymetry, with narrow valleys that rise from ocean floor (McDOUGALL 1985). The island sits on a shallow submarine platform, which then drops off to a depth of over 3000 m to meet the abyssal plain. Tutuila is approximately 32 km long, with a width that ranges

from less than 2 km to a maximum of 9 km. An insular shelf (<100 m depth) with an average width of 4 km extends along the entire north coast and the southwest region of the island (see Fig. 1).

The island is surrounded by fringing and barrier coral reefs, which contain a diversity of coral reef habitats, and coral species. The island has possibly subsided faster than coral reefs could grow upward, leaving former barrier reefs as submerged offshore banks along the seaward edges of the insular shelf (BIRKELAND *et al.* 2008). Fringing reefs have a width ranging from 0 to 600 m, but 90 % of them are less than 217 m (GELFENBAUM *et al.* 2011). The barrier reefs are located 2–3 km from the coastline. The total area of coral reefs in the territory of Tutuila is approximately 300 km².

2.2. The Samoa Event

The tsunami of September 29, 2009 earthquake was generated at the most active region of deep seismicity of Tonga Trench, and reached the Samoan island chain approximately 20 min later. The tsunami caused devastating property damage and loss of life on Tutuila island, because of its close proximity to the epicenter and the high population density on its coasts.

The cause of the earthquake was the rupture of a normal fault with a moment magnitude of $M_w = 8.1$ in the outer trench-slope at the north end of the trench, near the sharp bend to the west, followed by two inter-plate ruptures on the nearby subduction zone with moment magnitudes of $M_w = 7.8$ (LAY *et al.* 2010). Fault displacements measured by seismic signals (LAY *et al.* 2010), Global Positioning System (GPS) Stations, and ocean-bottom pressure sensors (BEAVAN *et al.* 2010) for these three separate faulting events support this picture. These fault displacements led to vertical movement of the seafloor, and created a complex tsunami source mechanism.

2.3. Observations

This particular tsunami afforded a unique opportunity to systematically evaluate the relationship between tsunami dynamics and coral reef damage. Six months prior to the tsunami, NOAA Coral Reef

Ecosystem Division (CRED)-certified divers performed comprehensive surveys of the reefs around Tutuila. The survey lines totaled 110 km in length. Observers measured the number of live, dead, and stressed corals, sea cucumbers, and urchins along track lines at the depths of 10–20 m. In the immediate aftermath of the tsunami the divers retraced most of the original survey lines. They documented clear evidence of fresh damage at depths between 10 and 20 m. This depth range was selected because of the location of the fore-reef at these depths, which is where the coral population is a maximum. Damage at depths shallower than 10 m was not recorded during the survey (BRAINARD *et al.* 2008).

The divers operated a tow board of instruments as it was tugged behind a boat at a depth of about 15 m. Data taken included direct observations from the diver, a downward facing camera and electronic instrumentation, including GPS (Fig. 2). The downward-pointed camera recorded the sea bottom habitat. It also captured images at 15 s intervals (NOAA-PIFSC-CRED unpublished data). Selected images of broken and overturned table corals and broken branching corals are presented in Fig. 2. The survey covered a total of 83 km linear distance within a 5 m horizontal zone either side of the track line. Divers were careful to try to differentiate between damage directly due to the tsunami itself, and land-originating debris entrained into the water.

The damage survey report synthesized the direct observations, aggregating track-line data into groupings based on 31 nearby villages, and reported the total number of damage observations (Table 3). The number of coral damage reports was supplemented with notes. Examples of such notes are: at Onenoa Village, “coral damage was low, with only one damaged tabulate *Acropora* sighting was recorded between both divers”; and at Amaluia Village it “consisted of isolated sightings of broken branching (species of *Pocillopora* and *Acropora*) corals”. The survey is not an absolute measure of coral damage and involves a degree of subjectivity: it records the number of observations of coral damage, not the absolute number of damaged corals. It is nonetheless a useful window onto the impact of tsunami dynamics in the immediate aftermath of the event. Since the full coral density of the island is not available, variation

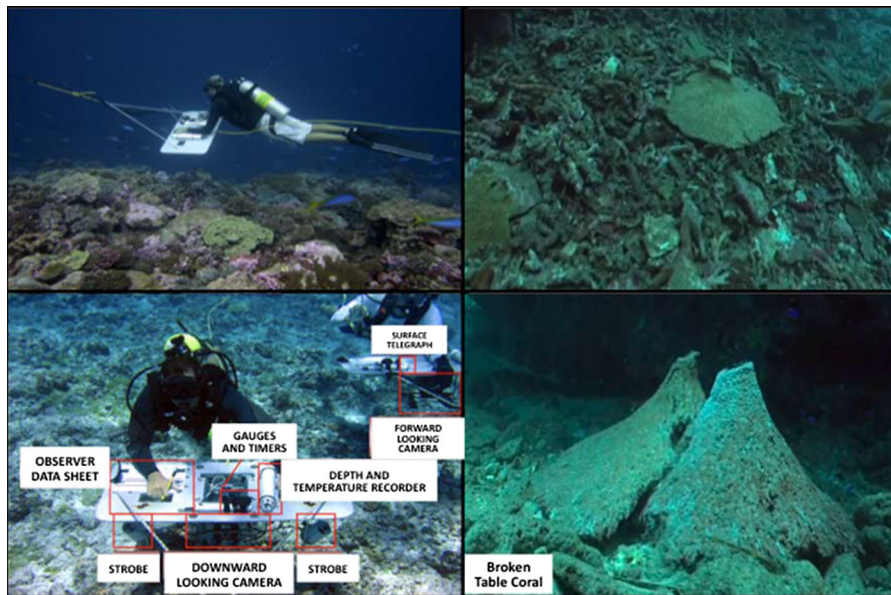


Figure 2

Photographs of the coral survey, methods and typical observations. *Upper left image* shows the NOAA-certified diver surveying a track line with a tow board tugged behind a boat. *Lower left image* shows the instrument suite on tow boards, among which are observer data sheet, gauges and timers, a camera and strobes. *Upper right* shows the table and branching corals that have been overturned; *lower right* shows a table coral that has been broken due to the tsunami. *Images* are taken from NOAA-Marine Debris Division

in coral density might influence the results (NOAA-PIFSC-CRED unpublished data).

The datasets reported by the divers for the number of damaged corals are discontinuous, unevenly and non-normally distributed, and this precludes classifying the coral damage observations with conventional methods such as standard deviation or equal intervals. Instead we used Jenks Natural Breaks classification method, a univariate version of k-means clustering (JENKS 1967) by sorting it from lowest value to highest and looking for large gaps, or natural breaks. This is done by seeking to minimize each class's average deviation from the class mean, while maximizing each class's deviation from the means of the other classes. In other words, the method iteratively seeks to reduce the variance within the same classes and maximize the variance between classes. The final classification in terms of coral damage is (0 no damage, 1–27 low, 38–63 medium, 83–159 high, 310 very high damage). While we felt the Jenks method is most appropriate for these data, our overall conclusions are not sensitive to this choice.

An international tsunami survey team observed and recorded tsunami run-up and inundation on the islands of the Samoan archipelago including Tutuila a week after the tsunami (FRITZ *et al.* 2011). The surveys followed the tsunami survey protocols reviewed by SYNOLAKIS and OKAL (2005). The team marked the values of run-up at 59 different field locations at Tutuila.

3. Modeling the Event

3.1. The Model Setup

We simulate the 2009 Samoa tsunami using the MOST Model (TITOV and GONZALEZ 1997). MOST is an established tsunami model that has been widely tested and evaluated, and it is used operationally for forecasting (e.g., TITOV 2009) and hazard assessment (e.g., TITOV *et al.* 2003). There are other numerical tsunami models with alternative dynamical equations and/or numerical schemes. Recognizing the importance for inter-model evaluations (SYNOLAKIS *et al.*

2008), recent community efforts have focused on using models that satisfy theoretical benchmarks and case study comparisons, such as those proposed by the National Tsunami Hazard Mitigation Program (NTHMP 2012). MOST meets the benchmarks and performs comparably to other tsunami models for the real-world case studies.

The primary metrics for comparison with observations are wave run-up and inundation. MOST solves the shallow water equations with a leapfrog finite difference scheme (TITOV and SYNOLAKIS 1998). We define three, nested bathymetric and topographic grids. The earthquake dislocation is input as the tsunami source; several predetermined tsunami

sources were tried in order to optimize the agreement with tide-gauge observations. Regional bathymetry and topography datasets (Table 1) were compiled and provided by National Geophysical Data Center (NGDC) and used to create the three nested grids (resolutions of 360, 60, and 10 m, respectively, see Fig. 3).

3.2. The Choice of Source Function

We simulated the 2009 Samoa Tsunami with a tsunami source function, f , calibrated to direct observations. For this event, several combinations of source functions f have been developed for use in

Table 1

Bathymetry compiled by NGDC to create the three nested grids (LIM et al. 2009)

Source of data	Production date	Data type	Horizontal and vertical datum	Spatial Resolution (m)
NGDC	1962–1998	Single beam echo-sounder	WGS-1984 and MHW	~100
NGDC	2009	Digitized coastline		30
NGDC	1996–2005	Multi-beam swath sonar		30–90
Gaia Geo-Analytical	2008	Estimated depths from satellite imagery		~5
NAVEOCEANO	2006	Bathymetric-topographic data		5
SCSC	2002	Vector data		10
USGS	1996–2006	NED digital elevation model		30

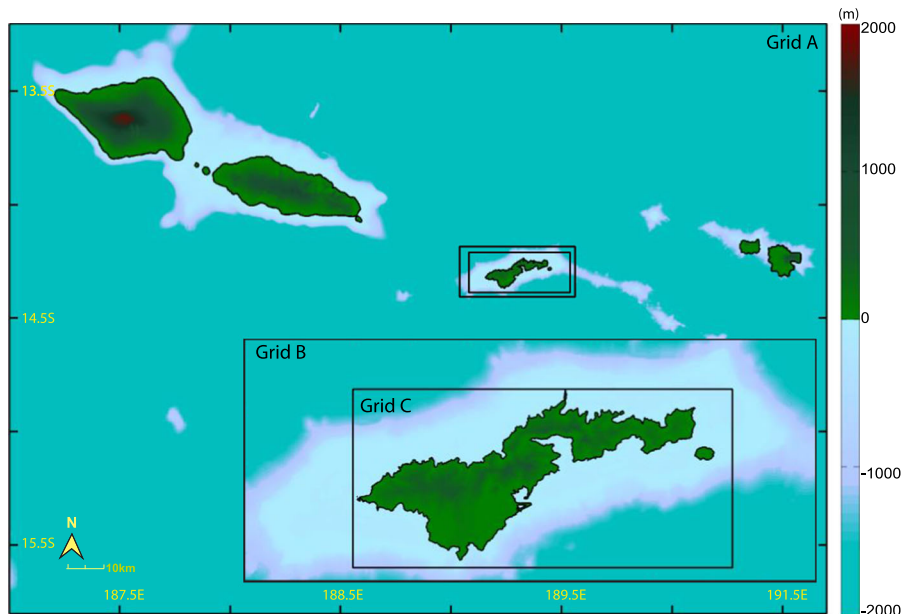


Figure 3

The boundaries of the nested A, B and C grids used in the MOST simulations

previous works (ZHOU *et al.* 2012; and TANG *et al.* 2009). Earthquakes are modeled as a combination of “unit sources”, S_1 , S_2 , S_3 and so on. Each unit source is a reverse thrust of a given strike, dip, and depth, and each has a moment magnitude of 7.5 (GICA *et al.* 2008). The parameters for these unit sources were chosen according to the inversion results of the method described in GICA *et al.* (2008). The tsunami source function f , is converted into an initial wave height using the elastic model of GUSYAKOV (1972). This assumes the rupture of rectangular fault planes causes vertical displacements of the sea floor, and that the initial water level movement is equal and instantaneous to the corresponding vertical sea-bottom displacement. The inversion finds the linear combination of unit sources that best matches the DART buoy data (PERCIVAL *et al.* 2009).

We tested four previously optimized source function f . Our choice of source function f was based on optimizing the agreement to the PagoPago tide gauge data. Of the source functions we considered, one significantly underestimated wave heights, the other three sources all performed comparably and performed well: for the first four waves, they all matched the tide-gauge wave amplitudes to within about 10 %, and the timing of crests and troughs to within 20 min. In order to make sure that our choice of source function was not being overfit to a single data point (PagoPago), we checked model output at a ‘virtual’ tide gauge at a model grid point west of the island. At this virtual tide gauge, the time series of wave height was robust to the choice of f . The outlier f for PagoPago remained an outlier, and there was close agreement among the other three f s. Although our results would

be similar for any of these three f s, we picked the source function with the best agreement to PagoPago (TANG *et al.* 2009) for which

$$f = 6.45 \times S_1 + 6.21 \times S_2, \quad (1)$$

where the specific parameters of S_1 and S_2 are given in Table 2.

3.3. Evaluation of the Model Results with DART and Tide Gauges

We first compare the tsunami wave amplitudes simulated with MOST to the tide-gauge observations in PagoPago in the near field and three DART Buoys 51425, 51426 and 54410 in the far field regions. For their locations, see Fig. 1. The simulated amplitudes match fairly well with the recorded values, particularly for PagoPago (Fig. 4), and particularly the first half-dozen fluctuations. The DART buoys record high-frequency crustal Rayleigh waves in the hour or so ahead of the arrival of the lower frequency tsunami waves (Fig. 5). Because the DART buoys lie farther from the source than Tutuila, phase discrepancies are expected to appear, which is particularly evident for DART Buoy 52425 (Fig. 5a). The discrepancies between the computed and recorded values at the DART buoys are likely also due to a secondary rupture occurred during the earthquake, which has been characterized in the model as one instantaneous rupture of the source function f . However, because of the excellent agreement with the PagoPago tide-gauge observations, we are confident these discrepancies are negligible for the purpose of run-up and inundation computations around Tutuila.

Table 2

Parameters of the two tsunami unit source functions, S_1 and S_2 (Eq. 1), used to simulate the 2009 Samoa tsunami

Unit Source	Longitude (°E)	Latitude (°S)	Dip (°)	Rake (°)	Strike (°)	Depth (m)	Mw	L (km)	W (km)	Slip (m)	Scaling parameter ()
1	187.2330	16.2754	9.68	90	182.1	5.00	8.1	100	50	1	6.45
2	187.8776	15.6325	57.06		342.4	6.57					6.21

4. Analysis

A comprehensive summary of data and analyses is presented in Table 3. We first evaluate whether there is any clear relationship between the two main observational datasets for this event—the coral damage and tsunami run-up for the 31 village sites. From Fig. 6 it is visually obvious that no such relationship exists ($r = 0.12$). Even excluding outliers

(13 m run-up, 100 damage numbers at Vaitogi, 5 m run-up and 310 damage numbers at Fagatele) the data still do not yield a clean story ($r = 0.18$). Across a range of run-ups between 2 and 8 m, coral damage is as likely to be low or very low, as it is to be high or very high.

We are obviously constrained by the limitations of the data that are available for analysis, but on this basis no clear relationship between observed run-up

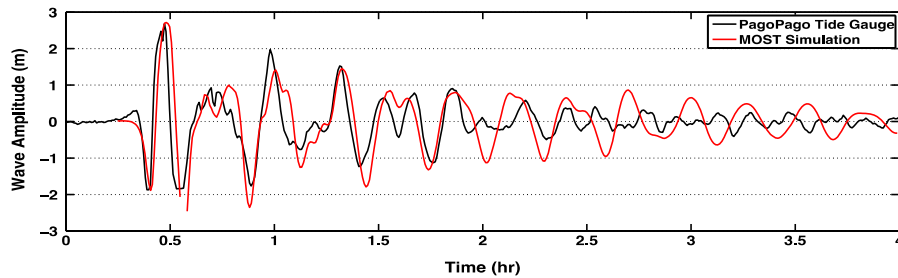


Figure 4

Comparison of observed (*black*) and simulated (*red*) water surface elevations at the PagoPago tide gauge (see Fig. 1) in the 4 h after the rupture at $t = 0$ (17:48:10 UTC, on Sep 29th, 2009). The MOST model estimated a maximum surface elevation of 2.3 m at the tide gauge, which agrees well with the recorded value

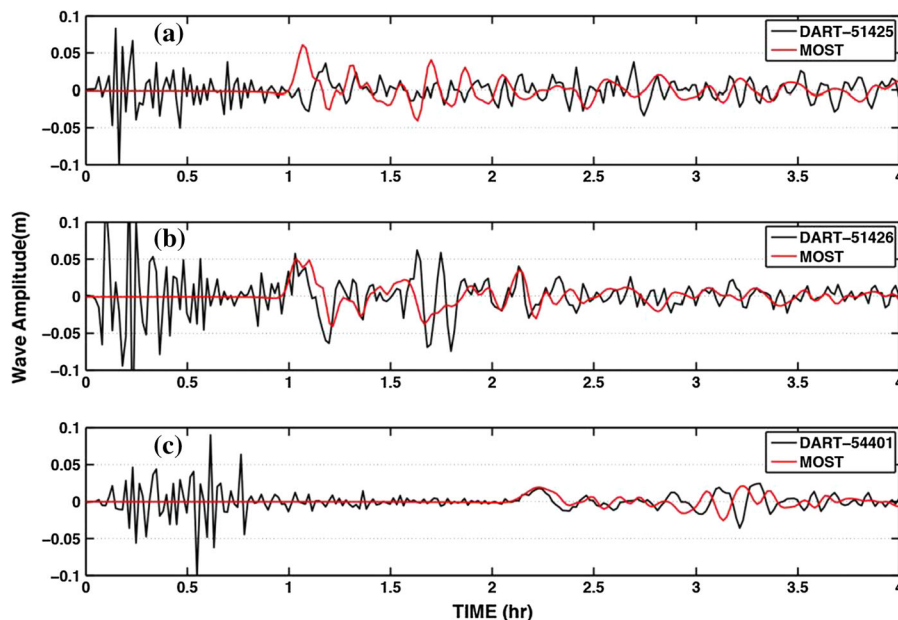


Figure 5

A comparison of the observed (*black*) and simulated (*red*) water surface elevations at three DART buoys, in the 4 h after the rupture at $t = 0$ (17:48:10 UTC on Sep 29th, 2009): **a** Buoy #51425, **b** Buoy #51426, and **c** Buoy #54401. High frequency, crustal Rayleigh waves are seen ahead of the arrival of the lower-frequency tsunami waves. The MOST model estimated maximum surface elevation of 0.05 m at selected DART locations

Table 3

Model, simulated and field run-up, differences, and coral damage at selected 31 villages around Tutuila

Village # (Fig. 1)	Village	Model run-up (m)	Field run-up (m)	Run-up difference (m)	Difference (%)	Average by village (%)	Coral damage	Coral dam. (numbers)
28	Afono1	3.52	4.31	-0.79	-18.33	-3.05	Medium	41
		3.6	4.08	-0.48	-11.76			
		3.9	4.41	-0.51	-11.56			
		3.4	3.75	-0.35	-9.33			
		3.69	3.59	0.1	2.79			
		3.05	2.59	0.46	17.76			
29	Afono2	3	2.25	0.75	33.33	38.43	Medium	41
		3.1	2.16	0.94	43.52			
10	Afao	4.2	5.89	-1.69	-28.69	-28.69	Low-medium	1
6	Agugulu	2.5	6.12	-3.62	-59.15	-59.15	High	86
30	Amalau	2.12	2.93	-0.81	-27.65	-19.45	No data	No data
		2.13	2.4	-0.27	-11.25			
4	Amanave	5.25	7.74	-2.49	-32.17	-32.17	High	151
11	Asilii	6	6.81	-0.81	-11.89	-11.89	Medium	42
12	Amaluia	5.2	5.39	-0.19	-3.53	-3.53	High	116
18	Amaua	3.2	2.91	0.29	9.97	9.97	No damage	0
19	Amouli	3.36	3.38	-0.02	-0.59	1.37	Low	13
		3.1	3	0.1	3.33			
24	Aoa	2.2	2.23	-0.03	-1.35	-1.35	No damage	0
21	Auasi	3.08	3.79	-0.71	-18.73	-18.73	Medium	38
20	Aunu'u	2.14	2.15	-0.01	-0.47	-0.47	High	121
16	Avaio	3.3	3.92	-0.62	-15.82	-3.36	Low	14
		3	2.75	0.25	9.09			
2	Fagailii	5.15	5.82	-0.67	-11.51	-18.82	No data	No data
		4.61	6.24	-1.63	-26.12			
31	Fagasa	4.2	4.13	0.07	1.69	1.69	No data	No data
1	Fagamalo	3	6.39	-3.39	-53.05	-48.71	No damage	0
		3.5	6.79	-3.29	-48.45			
		3.2	5.78	-2.58	-44.64			
14	Fagatele	3.3	4.92	-1.62	-32.93	-32.93	Very high	310
17	Fagaitua	4.75	3.5	1.25	35.71	59.77	No data	No data
		5	2.72	2.28	83.82			
5	Failolo	2.7	6.54	-3.84	-58.72	-58.72	High	159
13	Leone	2.65	2.75	-0.1	-3.64	67.86	High	83-116
		3.2	0.97	2.23	229.9			
		3.75	4.85	-1.1	-22.68			
27	Masefau	4	2.96	1.04	35.14	13.02	No data	No data
		4.4	4.84	-0.44	-9.09			
26	Masausi	3.15	2.79	0.36	12.9	12.9	No data	No data
9	Nua	4.2	4.09	0.11	2.69	2.69	No damage	0
23	Onenoa	2.6	2.74	-0.14	-5.11	-4.75	No damage	0
		2.4	2.51	-0.11	-4.38			
3	Poloa	7.6	17.59	-9.99	-56.79	-44.26	Low	24.00
		4.93	10.04	-5.11	-50.9			
		8	12.99	-4.99	-38.41			
		8.5	12.31	-3.81	-30.95			
25	Sailele	2.25	2.95	-0.7	-23.73	-23.73	Low	1
8	Seetaga	5.57	5.69	-0.12	-2.11	-2.11	Low	5
22	Tula	3.8	9.52	-5.72	-60.08	-40.87	Medium	63.00
		3.8	7.62	-3.82	-50.13			
		3.24	6.93	-3.69	-53.25			
		3.79	3.79	0	0			
7	Utumea	4	4.51	-0.51	-11.31	-11.31	Low	13
15	Vaitogi	1.8	3.36	-1.56	-46.43	-46.43	High	96

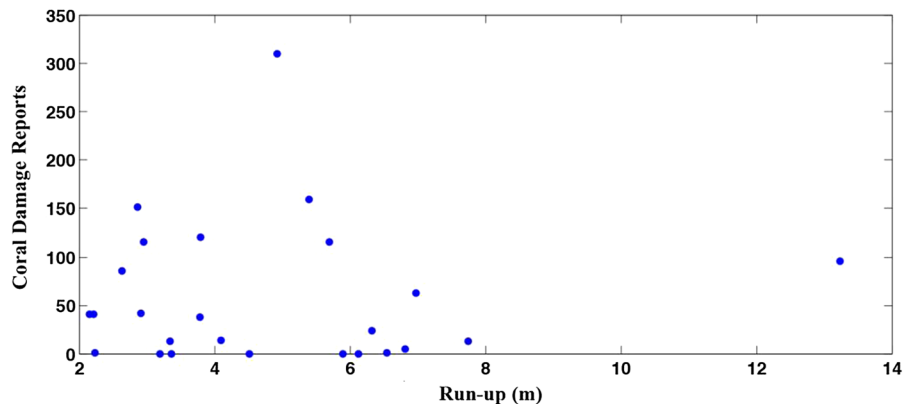


Figure 6

Coral damage vs. observational run-up. The *y*-axes shows coral damage numbers reported by the survey team, and the *y* axis is the average of the run-up observations after aggregating the data into 31 separate village locations (see Table 3; Fig. 1). There is no clear relationship between these two datasets

and coral damage can be inferred. It is not known whether this is because of limitations in the coral dataset (being only a sub-sampling of the reef environment), whether run-up is not the most relevant metric of tsunami dynamics, or whether the occurrence of coral damage is actually driven by many other unknown factors and antecedent conditions.

We next turn to a comparison of the observations with the MOST simulation of the event. We determined the run-up from MOST by taking the highest value of maximum wave amplitudes within a 3×3 grid box ($30 \text{ m} \times 30 \text{ m}$) around each of the 59 run-up data points.

We begin by presenting a comparison of the MOST simulations with observations for two representative locations. For the first (Fig. 7a) in the vicinity of the villages of Amaneve, Failolo, and Agugulu (4, 5, and 6 in Fig. 1), observed run-up averaged 8 m. For these villages, MOST does poorly, underestimating the run-up by an average of 45 %. This was a region where high coral damage was documented. For the second (Fig. 7b), near the villages of Utumea West, Nua and Seetaga (7, 8 and 9 in Fig. 1) average run-up was 4 m. Here MOST does well, simulating run-up to within 2.4 %. The documented coral damage was very low. Even though these two locations are only 3 km apart, these very

different run-ups, coral damage, and simulation performance illustrate the complexities of the setting.

Figure 8 shows some of the dynamical fields simulated by MOST for this event: maximum wave amplitude (panel a), maximum current (panel b), maximum flux (panel c) and peak stress (panel d), respectively, together with the coral damage along the survey tracks. From a visual analysis, there are not obvious strong relationships between coral damage and tsunami dynamical fields. Take just two examples, Leone and Fagatele (13 and 14 in Fig. 1): at Fagatele the maximum flux, current and maximum amplitudes are low, but coral damage is very high. In contrast, at Leone, the maximum flux is high with low maximum amplitudes and currents, and high coral damage.

The absence of a statistically significant relationship between the modeled tsunami fields and the observed damage is confirmed by averaging MOST output along each survey track and creating scatter plots of observed damage versus track-averaged model output, for several relevant model fields (see Fig. 11 in “Appendix”).

The clearest basis that we identify for comparing the observations and the model is the observed coral damage and run-up, and the simulated run-up, at each of the 31 sites where observations were made.

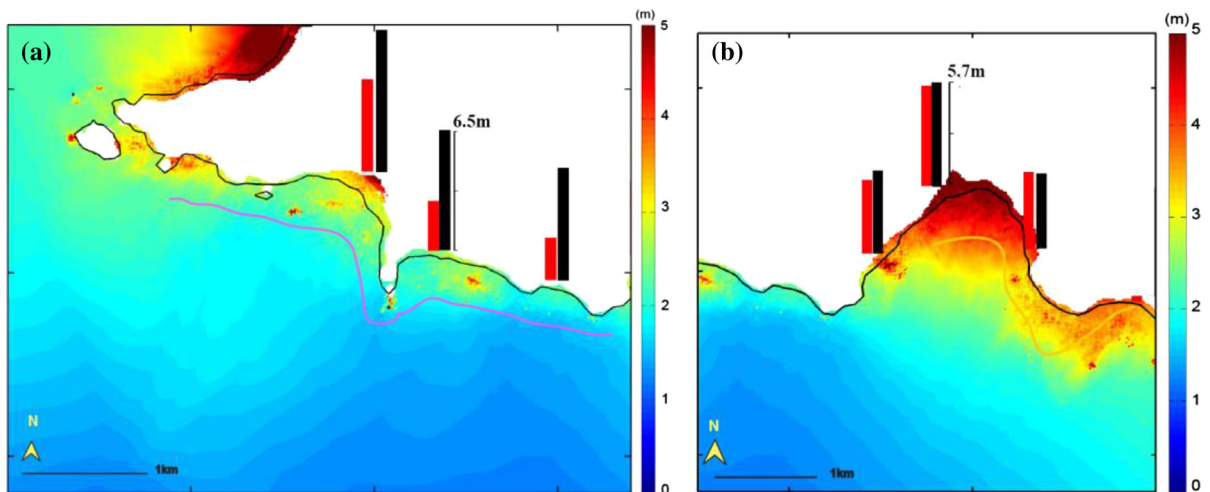


Figure 7

Two examples comparing observed run-up with MOST run-up and maximum wave height. Coastal run-up is shown as *black bars* (observed) and *red bars* (simulated). *Colors* show contours of maximum wave height simulated by MOST. **a** The villages of Amaneve, Failolo and Agugulu (locations 4,5, and 6 in Fig. 1; Table 3); **b** the village of Utumea West, Seetaga and Nua (locations 7, 8, and 9 in Fig. 1; Table 3) The survey tracks nearest these villages are also shown, *color-coded* according to damage scale in Fig. 10

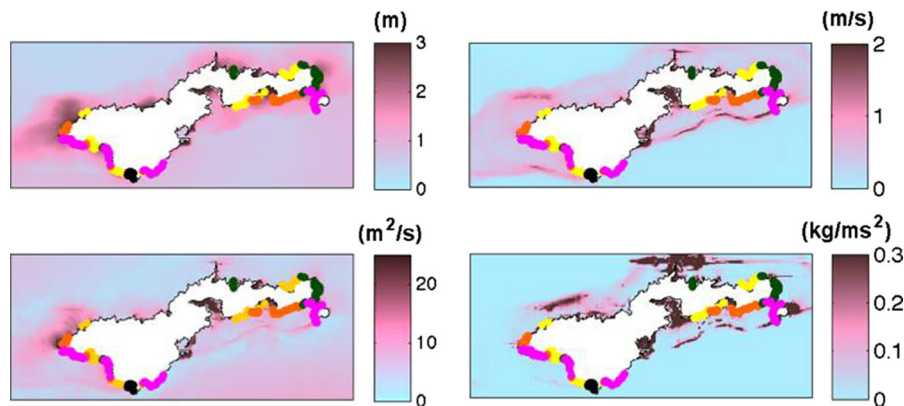


Figure 8

Maximum wave amplitudes, peak currents, peak fluxes and max, stresses calculated from the MOST simulation of the 2009 Tutuila tsunami. Also shown are the post-tsunami survey tracks with coral damage according to the *color scale* in Fig. 10

Table 3 compiles the complete results from all the available observations, We have aggregated the observed and computed run-up values into reports at 31 villages by taking the mean of the total data points at every village.

The complete dataset for the whole island is presented graphically in Figs. 9 and 10. A scatterplot of simulated versus observed run-up correlates at $r = 0.78$, demonstrating significant overall skill for the MOST model (Fig. 9). This overall level of

agreement between observations is comparable to other tsunami models and case studies (e.g., NTHMP 2012).

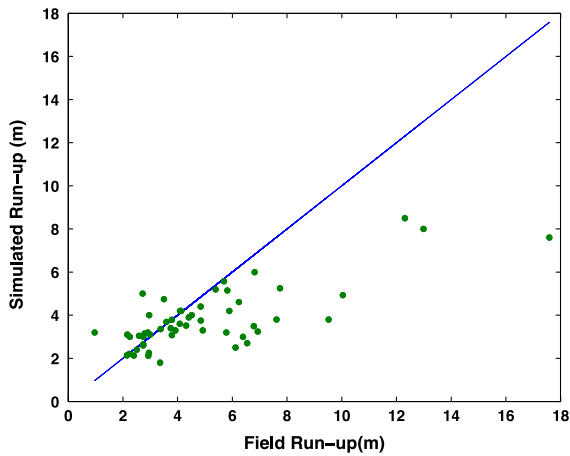


Figure 9

Scatter plot of simulated vs. observed run-up (m). The blue line shows the 1-to-1 line. The simulated vs. observed run-up is correlated at $r = 0.78$, but MOST underestimates run-up in many places

Despite this success, it is also clear MOST underestimates run-up in many places. Of the 31 total villages, there are 15 for which MOST underestimates run-up by more than 10 %. Figure 10 shows the bulk of these are on the west side of the island, although not exclusively so. At only 5 villages was the run-up overestimated by more than 10 %. Therefore, at the remaining 11 villages, the model simulated the observed run-up to within 10 %. Thus, while the nearby tide-gauge observations are well simulated by MOST (Fig. 4), there is an overall tendency for MOST to underestimate run-up for this event.

Turning to the coral damage reports for these villages, the data are suggestive of a general relationship with the accuracy of the run-up simulations (Table 3). Of the 15 villages where the model underestimated run-up, the breakdown in terms of coral damage is 8 very high/high, 4 medium, 3 low/very low, 1 no damage, 1 no data. For 11 villages where the model estimates run-up well, the coral damage is 2 very high/high, 1 medium, 3 low/very low, 4 no damage, 1 no data. For the 5 villages where

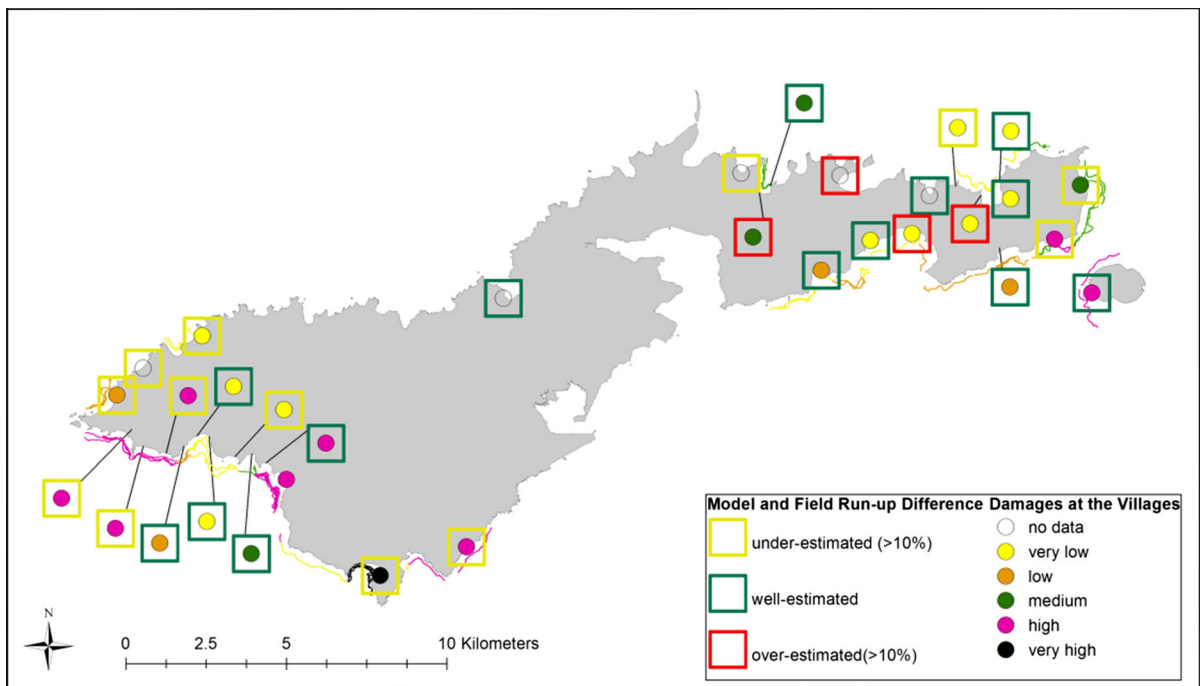


Figure 10

A summary of the comparison between model run-up skill and coral damage. Rectangles indicate the difference between modeled and observed run-ups. The filled dots indicate the coral damage reports using the qualitative classification described in the text. Lines are the colored survey track-lines followed to estimate the damage on corals. See also Table 3

run-up is overestimated, limited coral damage data preclude strong interpretation 1 high, 1 medium, 3 no data.

While these associations fall short of a formal, statistically significant correlation, there is an indication that at villages where MOST underestimates run-up, coral damage is much likely to be high or very high. It is interesting to speculate on whether there is a systematic reason for such associations, and whether it can be used to refine run-up dynamics. We turn to this in the discussion.

5. Summary and Discussion

Focusing on the impact of the 2009 Samoa tsunami on Tutuila island, we conducted numerical model simulations of tsunami run-up and inundation at the coastal zones. We performed an integrated analysis to evaluate the relationship between the tsunami hydrodynamics and the coral damage by using numerical modeling and post-tsunami surveys. The results for 31 villages on Tutuila island suggest that, while the numerical model simulates run-up with a high correlation with the observations, there is also a tendency to underestimate run-up in regions of high or very high coral damage, and that run-up tends to be better estimated in locations where coral damage is low.

The dataset synthesized in Table 3 is a preliminary assessment of the damage to the fringing reef coral. Although the 2009 Tutuila tsunami was a one-of-a-kind opportunity to investigate coral damage and tsunami dynamics, the data have some limitations. In particular, the damage assessments inevitably involve a degree of subjectivity and the damage reports have not been normalized to the background coral density. Moreover, the data cover only the east and west sides of Tutuila due to the bad weather conditions that existed on the south and north sides of the island during the surveys.

In the present setting of Tutuila island, the variable simulated run-up differences in our high-resolution tsunami model might be due to sharp changes in bottom roughness values caused by coral

reefs. One expects that in reality there are strong spatial variations in roughness values (NUNES and PAWLAK 2008). However, a constant roughness value was defined in the MOST simulations. This is a limitation and a standard practice shared by most current tsunami models. A productive direction for future research would be to implement spatially varying roughness, and to focus on detailed case studies of particular bays and reefs to understand how roughness variations affect run-up. Even though we used a very high-resolution model, for the Tutuila tsunami, there are significant differences from observations, and thus modeling this event remains a big challenge. A model sensitivity analysis simulating the effect of varying the depths where coral reefs exist may better elucidate their role in controlling run-up on the coastlines they shield.

While we have found some intriguing relationships between tsunami dynamics and coral damage, at least in the spatial variations in the skill of the numerical simulations, it is clear these are only tentative gleanings amid a great deal of variability. We did not find any clear relationships between coral damage and other simulated dynamical tsunami fields. Such relationships might be drawn out in more targeted and more detailed simulations, but the real situation is obviously very complicated at small scales, and many factors operate. The failure to establish a stronger connection between the simulated dynamical tsunami fields and coral damage may be because the coral damage dataset was not comprehensive enough; or because the MOST model does not represent the correct spatial scales in roughness or bathymetry, or MOST model does not represent the processes that actually cause damage (for instance, damage may be inflicted on corals by retreating waves carrying debris and sand); or because coral damage is inherently stochastic and unpredictable, and depends unknowably on antecedent conditions. Since so little is known about the damage to coral reefs by tsunamis, more studies are needed to examine the influence of water depth, three-dimensional effects, wave-wave interactions and coral strengths.

The role of reefs in tsunami dynamics remains enigmatic. Given the degree of complexity we found in both observations and simulations, it would, for instance, be hazardous to conclude that reefs provide universal protection for their inshore coastlines.

In some ways it is disappointing to find no correlation between the run-up and coral datasets. On the other hand, it is significant to establish that result, and it also points to new questions. The documentation of the submarine ecological impacts of a tsunami is an important goal in its own right, but the tentative inference from our study (the first of its kind) is that the relationship of coral damage to a variety of tsunami metrics (i.e., observed run-up and inundation, modeled maximum currents, fluxes, and stress) is not a simple one, at least in our setting. Tutuila represented a ‘target of opportunity’, since the all-important pre-tsunami survey existed. Alternative future surveying strategies range from identifying simpler bathymetric settings, more rigorous reporting protocols, or perhaps more comprehensive surveys in a smaller domain.

Would using a different mathematical model make a difference to our analyses? Some other tsunami models employ full three-dimensional Navier–Stokes equations (ABADIE *et al.* 2006) or Boussinesq approximations (KIRBY *et al.* 1998). However, bigger models do not always make for better models, and for long wavelength tsunamis shallow water equations have been shown to perform well in many benchmark problems and other comparisons. It is important to gauge the level of model complexity relative to other aspects of the problem. Key among these are: the uncertainty in the spatial roughness and the mathematical formulation of dissipation at small scales; the detailed bathymetry and coastal geometry at small scales, and how that interacts with the reflection and refraction of multiple wave fronts; and the intrinsic challenge of building numerical models of highly turbulent, chaotic, and one-off events with a single set of governing equations and parameters. As the situation stands, the advantages of each model class can be demonstrated under idealized circumstances,

but in inter-comparison studies all perform with comparable skill for real-world events (e.g., NTHMP 2012). As models are developed and refined, continued benchmarking and inter-model comparison will be essential to establish the strengths and ultimate limitations of each approach.

It is likely that the role of reefs depends sensitively on the detailed dynamics of any particular tsunami and the characteristics of the reefs themselves. This study is intended to contribute to the existing body of work on reef-tsunami interactions. It points to the need for more comprehensive research gathering more detailed coral damage data and testing the results with different case studies.

Acknowledgments

This publication makes use of data products provided by the Coral Reef Ecosystem Division (CRED), Pacific Islands Fisheries Science Center (PIFSC), National Marine Fisheries Service (NMFS), National Oceanic and Atmospheric Administration (NOAA), with funding support from the NOAA Coral Reef Conservation Program. NOAA Center for Tsunami Research under TSUNAMI TASK-2 Project, Pacific Marine Environmental Laboratory (contribution number 4368) supports this research. Hermann Fritz generously provided the post-tsunami run-up survey datasets. We are grateful to Randall Leveque, Joanne Bourgeois, Hongqiang Zhou, Yong Wei, Christopher Moore, Marie Eble, Diego Arcas and Lijuan Tang for their endless advice and their help.

Appendix

We construct scatterplots by averaging the MOST output for maximum amplitude, current, flux, and stress along each survey associated with a village (Fig. 1), and plotting against the corresponding observed coral damage numbers. None of the correlations are significant (Fig. 11).

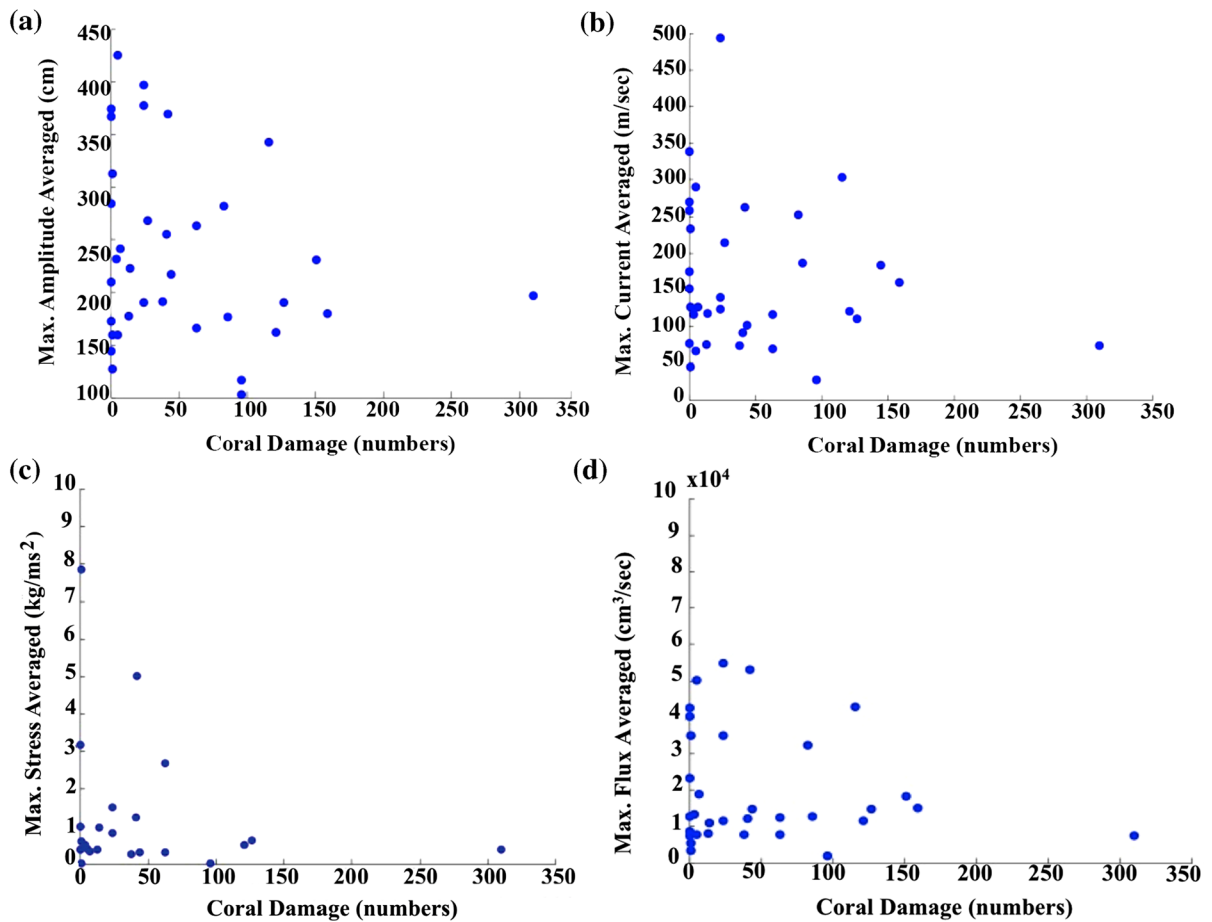


Figure 11

Scatter plots of coral damage (on the x -axis) vs. **a** maximum amplitude; **b** maximum current; **c** maximum flux and **d** maximum stress along coral damage track-lines. The dynamical fields are averaged over each track-lines associated with each village (Fig. 1), to evaluate any relationship between coral damage and dynamical fields

REFERENCES

- ABADIE S., GRILLI S., GLOCKNER S., (2006), A Coupled Numerical Model for Tsunami Generated by Subaerial And Submarine Mass Failures, In Proc. 30th Intl. Conf. Coastal Eng., San Diego, California, USA. 1420–1431.
- BABA T, MLECZKO R., BURBIDGE D., CUMMINS P., (2008), *The Effect of the Great Barrier Reef on the Propagation of the 2007 Solomon Islands Tsunami Recorded in Northeastern Australia*, Pure and Applied Geophysics, Vol. 165, 2003–2018.
- BAIRD A. H., CAMPBELL S. J., ANGGORO A. W., (2005), *Acehnese Reefs in the Wake of the Asian Tsunami*, Current Biology, Elsevier, Vol. 15, Issue 21, 1926–1930.
- BERGER M. J., and LEVEQUE R. J., (1998), *Adaptive Mesh Refinement Using Wave-Propagation Algorithms for Hyperbolic Systems*. SIAM J. Numer. Anal. 35, 2298–2316.
- BRAINARD R., ASHER J., GOVE J., HELYER J., KENYON J., MANCINI F., MILLER J., MYHRE S., NADON M., ROONEY J., SCHROEDER R., SMITH E., VARGAS-ANGEL B., VOGT S., VROOM P., BALWANI S., CRAIG P., DESROCHERS A., FERGUSON S., HOEKE R., LAMMERS M., LUNDBLAD E., MARAGOS J., MOFFITT R., TIMMERS M., VETTER O., (2008), U.S. Dept. of Commerce, National Oceanic and Atmospheric Administration, National Marine Fisheries Service.
- BEAVAN J., WANG X., HOLDEN C., WILSON K., POWER W., PRASETYA G., BEVIS M. and KAUTOKE R., (2010), *Near-simultaneous Great Earthquakes at Tongan Megathrust and Outer-rise in September 2009*, Nature., Vol. 466. doi:10.1038/nature09292.
- BIRKELAND C., CRAIG P., FENNER F., SMITH L., KIENE W. E. and RIEGL B., (2008), *Geologic Setting and Ecological Functioning of Coral Reefs in AS*. Coral reefs of the USA, Springer Publishers, Chap. 20, Vol. 33, 803.
- CHATENOUX B., PEDUZZI P., (2007), *Impacts from the 2004 Indian Ocean Tsunami: Analyzing the Potential Protecting Role of Environmental Features*, Natural Hazards, Vol. 40, 289–304.
- DRAPER N. R., SMITH H., (1998), Applied Regression Analysis (3rd ed.). Wiley, New York.

- FERNANDO H. J. S., (2005), *Coral Poaching Worsens Tsunami Destruction in Sri Lanka*, *Eos*, Vol. 86, No. 33.
- FERNANDO H. J. S., SAMARAWICKRAMA S. P., BALASUBRAMANIAN S., HETTIARACHCHIB S. S. L., VOROPAYEVA S., (2008), *Effects of Porous Barriers Such as Coral Reefs on Coastal Wave Propagation*, *Journal of Hydro-environment Research*, Elsevier, Vol. 1, Issues 3–4, 187–194.
- FRTZ H. M., BORRERO J. C., SYNOLAKIS C. E., OKAL E. A., WEISS R., LYNETT P. J., TITOV V. V., FOTEINIS S., JAFFE B. E., LIU P. E., and CHAN C., (2011), *Insights on the 2009 South Pacific Tsunami in Samoa and Tonga from Field Surveys and Numerical Simulations*, *Earth Sci. Rev.*, Vol. 107, 66–75. doi:[10.1016/j.earscirev.2011.03.004](https://doi.org/10.1016/j.earscirev.2011.03.004).
- GELFENBAUM, G., APOSTOS, A., STEVENS, A. W., JAFFE, B., (2011), *Effects of fringing reefs on tsunami inundation: American Samoa*, *Earth-Science Reviews*, Vol. 107, 12–22.
- GICA, E., SPILLANE, M. C., TITOV, V. V., CHAMBERLIN, C. D., and NEWMAN, J. C., (2008), *Development of the forecast propagation database for NOAA's Short-term Inundation Forecast for Tsunamis (SIFT)*, NOAA Tech. Memo. OAR PMEL-139, 89.
- GUSYAKOV, V. K., (1972), *Mathematical problems of geophysics, chapter Generation of tsunami waves and ocean Rayleigh waves by submarine earthquakes*, Vol. 3, Novosibirsk, VZ SO AN SSSR, 250–272.
- JENKS G. F., (1967), *The Data Model Concept in Statistical Mapping*, *International Yearbook of Cartography*, Vol. 7, 186–190.
- KIRBY J., WEI G., CHEN Q., KENNEDY A., DALRYMPLE R., (1998), FUNWAVE 1.0, Fully Nonlinear Boussinesq Wave Model Documentation and Users Manual. Tech. Rep. Research Report No. CACR-98-06, Center for Applied Coastal Research, University of Delaware.
- KUNKEL M., HALLBERG R. W., OPPENHEIMER M., (2006) *Coral reefs reduce tsunami impact in Model Simulations*, *Geophysical Research Letters*, Vol. 33, 123612. doi:[10.1029/2006GL027892](https://doi.org/10.1029/2006GL027892).
- LIM E., TAYLOR L. A., EAKINS B. W., CARIGNAN K. S., WARNKEN R. R., GROTHE P. R., (2009), *Digital Elevation Models of Craig, Alaska: Procedures, Data Sources and Analysis*. NOAA Technical Memorandum NESDIS NGDC-27.
- LAY T., AMMON C. J., KANAMORI H., RIVERA L., KOPER K. D., HUTKO A. R., (2010), *The 2009 Samoa–Tonga Great Earthquake Triggered Doublet*, *Nature*, Vol. 466, 964–968. doi:[10.1038/nature09214](https://doi.org/10.1038/nature09214).
- MCDUGALL I., (1985), *Age and Evolution of the Volcanoes of Tutuila*, *American Samoa Pacific Science*, Vol. 39, No:4.
- NATIONAL TSUNAMI HAZARD MITIGATION PROGRAM, (NTHMP), (2012). *Proceedings and Results of the 2011 NTHMP Model Benchmarking Workshop*. Boulder: U.S. Department of Commerce/NOAA/NTHMP; (NOAA Special Report). 436.
- NUNES V. and PAWLAK G., (2008), *Observations of bed roughness of a coral reef*, *Journal of Coastal Research*, 24(2B), 39–50, West Palm Beach (Florida), ISSN 0749-0208.
- OKADA Y., (1985), *Surface Deformation due to Shear and Tensile Faults in a Half-Space*, *Bulletin of the Seismological Society of America*, Vol. 75 (4), 1135–1154.
- OKAL E., BORRERO J. C., CHAGUE-GOFF C., (2011), *Tsunamiogenic Predecessors to the 2009 Samoa Earthquake*, *Earth–Science Reviews*, Vol. 107, 128–140.
- OKAL E. A., FRITZ H. M., SYNOLAKIS C. E., BORRERO J. C., WEISS R., LYNETT P. J., TITOV V. V., FOTEINIS S., JAFFE B. E., CHAN C., LIU P. E., (2010), *Field Survey of the Samoa Tsunami of 29 September 2009*, *Seismol. Res. Lett.*, Vol. 81 (4), 577–591.
- PERCIVAL D. B., ARCAS D., DENBO D. W., EBLE M. C., GICA E., MOFJELD H. O., SPILLANE M. C., TANG L., TITOV V. V., (2009), *Extracting tsunami source parameters via inversion of DART® buoy data*. NOAA Tech. Memo. OAR PMEL-144, 22.
- ROEBER V., YAMAZAKI Y., CHEUNG K. F., (2010), *Resonance and Impact of the 2009 Samoa Tsunami Around Tutuila*, *American Samoa*, *Geophys. Res. Lett.*, Vol. 37, 121604. doi:[10.1029/2010GL044419](https://doi.org/10.1029/2010GL044419).
- SYNOLAKIS C. E., OKAL E. A., (2005), *1992–2002 Perspective on a Decade of Post Tsunami Surveys*, *Adv. Nat. Technol. Hazards*, Vol. 23, 1–30. doi:[10.1007/1-4020-3331-1_1](https://doi.org/10.1007/1-4020-3331-1_1).
- SYNOLAKIS, C.E., BERNARD E., TITOV V. V., KANOĞLU U., and GONZÁLEZ F. I., (2008), *Validation and Verification of Tsunami Numerical Models*. *Pure Appl. Geophys.*, 165(11–12), 2197–2228.
- TANG L., TITOV V. V., CHAMBERLIN C. D., (2009), *Development, testing, and applications of site-specific tsunami inundation models for real-time forecasting*. *J. Geophys. Res.*, 114, C12025. doi:[10.1029/2009JC005476](https://doi.org/10.1029/2009JC005476).
- TERRY J. P., KOSTASCHUK R. A., GARIMELLA S., (2005), *Sediment deposition rate in the Falefa River basin, Upolu Island, Samoa*, *Journal of Environmental Radioactivity*, Vol. 86(1), 45–63.
- TITOV, V. V., (2009), *Tsunami Forecasting*. Chapter 12 in *The Sea*, Vol. 15: *Tsunamis*, Harvard University Press, Cambridge, MA and London, England, 371–400.
- TITOV V. V., and SYNOLAKIS C., (1998), *Numerical Modeling of Tidal Wave Runup*, *Journal Of Waterway, Port, Coastal, And Ocean Engineering*, Vol. 124(4), 157–171.
- TITOV, V. V., and GONZALEZ, F. I., (1997), *Implementation and Testing of the Method of Splitting Tsunami (MOST) Model*, NOAA Tech. Memo. ERL PMEL-112, NTIS:PB98-122773.
- TITOV, V.V., F.I. GONZÁLEZ, H.O. MOFJELD, and A.J. VENTURATO, (2003), *NOAA TIME Seattle Tsunami Mapping Project: Procedures, Data sources, and Products*. NOAA Tech. Memo. OAR PMEL-124, NTIS: PB2004-101635, 21.
- ZHOU H., WEI Y., TITOV V. V., (2012), *Dispersive Modeling of the 2009 Samoa Tsunami*, *Geophysical Research Letters*, Vol. 39, L16603. doi:[10.1029/2012GL053068](https://doi.org/10.1029/2012GL053068).